





Received 18 January 2024; revised 8 April 2024; accepted 8 May 2024; date of publication 10 May 2024;  
date of current version 29 May 2024.

Digital Object Identifier 10.1109/TQE.2024.3399609

# Reliable Quantum Communications Based on Asymmetry in Distillation and Coding

LORENZO VALENTINI<sup>1</sup>  (Graduate Student Member, IEEE),  
RENÉ BØDKER CHRISTENSEN<sup>2,3</sup> , PETAR POPOVSKI<sup>3</sup>  (Fellow, IEEE),  
AND MARCO CHIANI<sup>1</sup>  (Fellow, IEEE)

<sup>1</sup>CNIT/WiLab, DEI, University of Bologna, 40126 Bologna, Italy

<sup>2</sup>Department of Mathematical Sciences, Aalborg University, 9220 Aalborg, Denmark

<sup>3</sup>Department of Electronic Systems, Aalborg University, 9220 Aalborg, Denmark

Corresponding author: Lorenzo Valentini (e-mail: lorenzo.valentini13@unibo.it).

This work was supported in part by the Villum Investigator Grant “WATER” from the Velux Foundations, Denmark and in part by the European Union—Next Generation EU, PNRR Project, Italy, under Grant 2022JES5S2.

**ABSTRACT** The reliable provision of entangled qubits is an essential precondition in a variety of schemes for distributed quantum computing. This is challenged by multiple nuisances, such as errors during the transmission over quantum links, but also due to degradation of the entanglement over time due to decoherence. The latter can be seen as a constraint on the latency of the quantum protocol, which brings the problem of quantum protocol design into the context of latency–reliability constraints. We address the problem through hybrid schemes that combine: indirect transmission based on teleportation and distillation, and direct transmission, based on quantum error correction (QEC). The intuition is that, at present, the quantum hardware offers low fidelity, which demands distillation; on the other hand, low latency can be obtained by QEC techniques. It is shown that, in the proposed framework, the distillation protocol gives rise to asymmetries that can be exploited by asymmetric quantum error correcting code, which sets the basis for unique hybrid distillation and coding design. Our results show that ad hoc asymmetric codes give, compared with conventional QEC, a performance boost and codeword size reduction both in a single-link and in a quantum network scenario.

**INDEX TERMS** Asymmetric channels, asymmetric quantum error correction (QEC), entanglement, quantum communication, quantum distillation.

## I. INTRODUCTION

The evolution of the quantum Internet happens in symbiosis with classical communication and the existing Internet technology, leading to a number of interesting research challenges [1], [2], [3]. There are two principal types of applications for quantum communication: (a) enhancing already existing services, such as quantum key distribution [4] or super-dense coding [5] and (b) enabling new services, such as distributed quantum computing [6], [7], [8] or remote processing of quantum sensing data [9], [10]. The applications in (a) convey classical information, while the applications in (b) convey quantum information. A quantum network can be defined as a collection of nodes, which are able to exchange qubits and distribute entangled states among the network nodes [11]. Two possible ways to exchange quantum

information are the indirect transmission through quantum teleportation protocol [12], and direct transmission of qubits exploiting quantum error correction (QEC) [13].

For *indirect transmission*, the key building block to achieve reliable communication over teleportation is the distribution of Einstein–Podolsky–Rosen (EPR) entangled pairs or other types of entangled states [14], [15], [16]. Since such a distribution is affected by imperfections [17], [18], [19], [20], [21], [22], distillation protocols [23], [24] have been developed to increase the fidelity of the shared EPR pairs. In this way, it is possible to make the communication reliable at the cost of an increase in both latency and usage of qubit resources.

There are the following three basic schemes for heralded entanglement generation [25]:

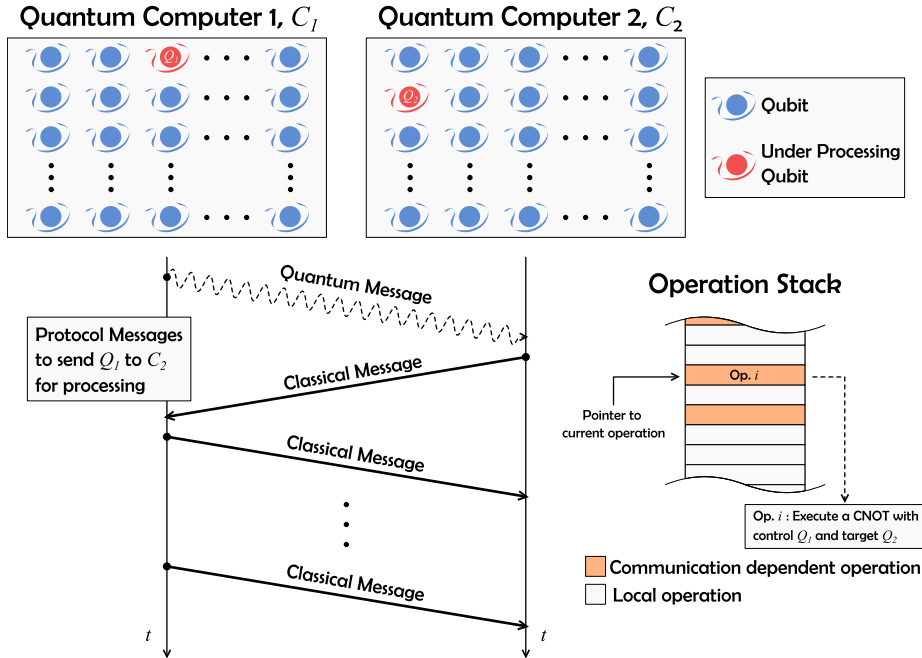


**FIGURE 1.** Motivating example of distributed quantum computation. Two quantum computers  $C_1$  and  $C_2$  share a common task represented by a sequential operation stack. Following certain scheduling related to the computation, whenever two qubits of different quantum computers require an interaction, a quantum communication link is used to send one of these qubits to the other, execute the operation, and send it back.

- 1) *at source*, where the transmitter is in charge of generating and sharing the entanglement;
- 2) *at mid-point*, where the entanglement source is in between the transmitter and the receiver;
- 3) *at both end-points*, where the entanglement sharing is addressed cooperatively by the transmitter and receiver.

These schemes have resulted in several proposals for quantum Internet protocol stacks. For example, in [26], a protocol stack based on *at source* distribution was proposed, while in [27] and [28], the authors worked with distribution based on *at both end-points*.

The toy example from Fig. 1 features an indirect communication among two quantum computers using *at source* entanglement distribution. In particular, the timing diagram of Fig. 1 illustrates the overall latency for sending a qubit  $Q_1$  from a quantum computer  $C_1$  to another computer  $C_2$ . First, a quantum message is sent from  $C_1$  to  $C_2$ , containing a number of qubits (halves of EPR pairs). Due to noise, the shared pairs will typically no longer be fully entangled, and therefore not suitable to be used directly for teleportation. Thus, a chain of classical messages is exchanged to improve the reliability of the pairs, according to distillation protocols [23]. On the flip side, this exchange of messages will also increase the overall latency. Finally, a (classical) teleportation message is sent to convey the quantum information. Note that, due to decoherence, the fidelity of the shared pairs will degrade over time; this is modeled as a constraint on the protocol latency.

For the example in Fig. 1, *reliability* is the ability to preserve the transmitted state along the path to the receiver, while *latency* is the time between the intention to transmit a qubit and its actual reception. Suppose that one has to execute a quantum algorithm involving many qubits, such as in the factoring algorithm [29]. We recall that any quantum computation can be implemented by adopting a finite set of universal quantum gates, operating on one or two qubits. The possible scheduling of operations is represented by the stack in Fig. 1. When the quantum memory of a single quantum computer is not sufficient for the algorithm, we could consider exploiting multiple quantum computers, for example, two of them are indicated as  $C_1$  and  $C_2$  in Fig. 1. In order to perform double qubit operators in a distributed manner, the two quantum computers should be able to reliably exchange qubits. Assume that, at a given time, a qubit  $Q_1$  of  $C_1$  has to interact with a qubit  $Q_2$  of  $C_2$ . Thus,  $C_1$  sends its qubit to  $C_2$  using an indirect communication based on distillation and teleportation as previously discussed (see also the timing diagram). Computer  $C_2$  may now execute the local operation on  $Q_1$  and  $Q_2$ . We note that a higher reliability constraint demands a larger number of distillation (classical) messages, resulting in increased latency of the communication protocol and directly affecting the algorithm's computational time. Note that reliability constraint is crucial since communication errors lead to reset/restart of the algorithm from the beginning. From this simple example, we find a motivation to search for strategies reaching the same reliability as the distillation protocol, while minimizing the number of exchanged classical messages.

Regarding *direct* communication, Fowler et al. [13] considered a quantum link in which the information qubits are conveyed by surface codes [30], [31], [32]. When QEC is present, it is also possible to piggyback classical information over quantum information [33]. In general, we can classify quantum error correcting code (QECC) into symmetric [34], [35], [36] and asymmetric [37], [38]. A symmetric  $[[n, k, d]]$  quantum error correcting code (QECC) encodes  $k$  information qubits into  $n$  physical qubits and is able to correct up to  $t = \lfloor (d - 1)/2 \rfloor$  generic errors (i.e., Pauli  $X$ ,  $Z$ , or  $Y$ ) on the coded qubits. On the other hand, an asymmetric  $[[n, k]]$  QECC with  $(e_g, e_z)$  error correction capability [38] is able to correct up to  $e_g$  generic errors and  $e_z$  particular errors, in this case Pauli  $Z$  ones. Other asymmetric codes can be defined as  $[[n, k, d_X/d_Z]]$  due to the fact that they are able to correct  $t_X = \lfloor (d_X - 1)/2 \rfloor$  Pauli  $X$  errors and  $t_Z = \lfloor (d_Z - 1)/2 \rfloor$  Pauli  $Z$  errors (e.g., Calderbank–Shor–Steane codes [37], [39], [40], [41]). In quantum communication, given a fixed error probability on the transmitted qubits, QEC-based communication schemes provide higher reliability than uncoded schemes, whenever the initial error probability is below a certain code-dependent threshold. In general, this initial error probability is termed *fidelity* and is technology dependent. Furthermore, in direct communication protocols, reliability comes at the cost of quantum memory size through coding.

This idea to subdivide quantum communication protocols into direct and indirect ones also appears in [42], where networks are categorized into “generations” based on the employed error management scheme. Some of them deal with errors by the means of distillation, others using QEC. In this context, we locate this article in between these two kinds of generations and investigate hybrid schemes adopting both distillation and QEC techniques. In particular, we assume that local errors (i.e., quantum gate errors and quantum measurements) are negligible compared with nonlocal errors (i.e., fidelity reduction due to transmission). In such a scenario, direct communication is not yet feasible, but at each node of the network, QEC can be exploited. The justification of using QEC schemes (both hybrid or purely QEC based) is the latency reduction that can be obtained compared with uncoded ones. In fact, to achieve the same target reliability, the uncoded scheme requires more distillation steps, expressed as transmissions of classical messages. On the other hand, it is also possible to fix the latency by presetting the number of distillation steps and obtain a gain in reliability using QECCs. Furthermore, in this new framework, we point out that the distillation protocol gives rise to asymmetries, which can be exploited by asymmetric QECCs [37], [38], and therefore, we can have a joint distillation and coding design. Besides the discussed example in Fig. 1, applications can be represented by mid-generation error management schemes for quantum Internet, adaptive QEC for reliable communication over quantum networks, multicore quantum computing [6], construction of quantum graph state [43], [44], [45] over networks, and many others.

The key contributions of this article can be summarized as follows:

- 1) proposal of a hybrid distillation-QEC scheme, which exploits the asymmetries arising from distillation protocols;
- 2) evolution analysis of the equivalent quantum channel parameters of a distillation protocol to find out exploitable asymmetries;
- 3) proposal and design of an improved quantum network protocol based on scheduling policies for swapping and distillation;
- 4) demonstration that ad hoc asymmetric codes can provide, compared with conventional QEC, a performance boost and codeword size reduction both in a single-link and in a network scenario.

The rest of this article is organized as follows. Section II introduces preliminary concepts and models together with some background material. Section III focuses on the main contributions of this article. Numerical results are shown in Section IV. Finally, Section VI concludes this article.

*Notations:* Throughout this article, capital bold letters denote matrices. We adopt the bra-ket notation to indicate vectors representing quantum states. The ket vector  $|\psi\rangle$  is a column vector with complex coefficients, while the bra vector  $\langle\psi|$  is its complex conjugate.

## II. PRELIMINARIES AND BACKGROUND

A qubit is an element of the 2-D Hilbert space  $\mathcal{H}^2$ , with orthonormal basis  $|0\rangle$  and  $|1\rangle$  [46], [47]. The Pauli operators  $I$ ,  $X$ ,  $Z$ , and  $Y$  are defined by  $I|a\rangle = |a\rangle$ ,  $X|a\rangle = |a \oplus 1\rangle$ ,  $Z|a\rangle = (-1)^a |a\rangle$ , and  $Y|a\rangle = i(-1)^a |a \oplus 1\rangle$  for  $a \in \{0, 1\}$ , where  $\oplus$  is the XOR operation. These operators either commute or anticommute with each other. Other useful single qubit gates, which are used in this article, are the Hadamard gate described as  $H = (X + Z)/\sqrt{2}$  and the  $x$ -axis rotation gate  $R_x(\theta) = \cos(\theta/2)I - i \sin(\theta/2)X$ . We use the notation  $|\Phi^\pm\rangle = (|00\rangle \pm |11\rangle)/\sqrt{2}$  and  $|\Psi^\pm\rangle = (|01\rangle \pm |10\rangle)/\sqrt{2}$  for two-qubit Bell’s states or, equivalently, EPR pairs. A CNOT gate is a quantum gate that acts on two qubits, one referred to as *control* and the other as *target*. In particular, if the control qubit is in state  $|1\rangle$ , then the target qubit is inverted, otherwise, nothing happens according to  $|c\rangle|t\rangle \mapsto |c\rangle|t \oplus c\rangle$ . Considering an  $n$ -qubit system, we indicate with  $Z_j$  a Pauli  $Z$  operator acting on the  $j$ th qubit. Similarly for a CNOT gate, with  $CX_{j,k}$ , we indicate that the operator has the  $j$ th qubit as control and the  $k$ th qubit as target. We define a mixed state as a distribution over quantum states,  $\{p_i, |\psi_i\rangle\}$ , meaning that with probability  $p_i$  the system is in state  $|\psi_i\rangle$ . We represent the state of the quantum system using the density matrix representation  $\rho = \sum_i p_i |\psi_i\rangle \langle\psi_i|$ .

The quantum teleportation protocol is an algorithm that transfers a quantum state from one qubit to another at the cost of two classical bits and an EPR pair [12]. The procedure can be summarized as follows:

- 1) prepare a three-qubit state in  $|\psi\rangle|\Phi^+\rangle$ ;
- 2) apply  $H_1CX_{1,2}$ ;
- 3) measure the first and the second qubit in the  $\{|0\rangle, |1\rangle\}$ -basis;
- 4) based on the results of the measurements  $(m_1, m_2) \in \{0, 1\}^2$ , apply  $X_3^{m_2}Z_3^{m_1}$  to obtain  $|\psi\rangle$  on the third qubit.

Since the first operation acts only on the first two qubits, it is possible to transfer an unknown quantum state at distance having a preshared EPR pair and transmitting two bits of information over a classical channel.

### A. QUANTUM DISTILLATION PROTOCOLS

In order to reliably teleport a quantum state it is assumed to have a perfect preshared EPR pair  $|\Phi^+\rangle$ . However, imperfect local operations and entanglement generation at distance induce errors on the preshared pair, which lead to mixed states. We describe the mixed state with the density matrix

$$\begin{aligned} \rho = & A|\Phi^+\rangle\langle\Phi^+| + B|\Psi^-\rangle\langle\Psi^-| \\ & + C|\Psi^+\rangle\langle\Psi^+| + D|\Phi^-\rangle\langle\Phi^-| \end{aligned} \quad (1)$$

where the coefficients are real, normalized  $A + B + C + D = 1$ , and defined on the interval  $[0, 1]$ . The coefficient  $A$  is the entangled pair fidelity. An important mixed state is the maximally mixed one, referred to in the following as a Werner state [23], [48], [49], having density matrix:

$$\begin{aligned} \rho = & \mathcal{F}|\Phi^+\rangle\langle\Phi^+| + \frac{1-\mathcal{F}}{3} [|\Psi^-\rangle\langle\Psi^-| \\ & + |\Psi^+\rangle\langle\Psi^+| + |\Phi^-\rangle\langle\Phi^-|] . \end{aligned} \quad (2)$$

Several techniques have been developed to increase the fidelity of entangled states for teleportation. Here, we consider the distillation algorithm presented in [24], which improves [23]. The distillation protocol can be summarized as follows [50]:

- i) share two EPR pairs (i.e., first pair: qubits 1 and 2, second pair: qubits 3 and 4), both in state (1);
- ii) apply the local rotations  $R_{x_1}(\pi/2)R_{x_2}(-\pi/2)R_{x_3}(\pi/2)R_{x_4}(-\pi/2)$ ;
- iii) apply the local CNOTS  $CX_{1,3}CX_{2,4}$ ;
- iv) measure qubits 3 and 4 and share via classical messages the measurement information;
- v) if the measurements agree (i.e., both 0 s or 1 s) keep the final pair, otherwise discard it.

Through this article, we consider that errors in quantum measurements, quantum local operations, and classical communications can be neglected. In [51], [52], and [53], some of these aspects have been accounted for, although not adopting [24], which is our focus in this work. Since the procedure from ii) to iv) uses only local operations and measurements, these steps can be efficiently pipelined to minimize the latency of the communication protocol [26]. A pictorial representation of the distillation procedure is provided in



**FIGURE 2.** Pictorial representation of raw entanglement distribution and one step of entanglement distillation. In this example, the transmitter attempts to share 13-qubits, where each of them is part of a different Einstein–Podolsky–Rosen (EPR) pair. The receiver successfully detects seven qubits among the 13 transmitted ones. It groups three pairs for distillation, performs it, and discards the unpaired one. Finally, it sends the information about which qubit has to be kept and measurements to the original transmitter. Concluding the distillation procedure in this example, we have two EPR pairs in position 1 and 8 of the user’s respective quantum memories.

Fig. 2 . The resulting mixed state, considering equally distributed EPR pairs (also referred as symmetric distillation), is described by

$$\begin{aligned} A_{i+1} &= (A_i^2 + B_i^2) N_i^{-1} \\ B_{i+1} &= 2C_i D_i N_i^{-1} \\ C_{i+1} &= (C_i^2 + D_i^2) N_i^{-1} \\ D_{i+1} &= 2A_i B_i N_i^{-1} \end{aligned} \quad (3)$$

where the subscripts indicate the number of distillation steps and  $N_i = (A_i + B_i)^2 + (C_i + D_i)^2$  is a normalization factor. The convergence of (3) to  $A_i \rightarrow 1$  when  $i \rightarrow \infty$  was proven in [54]. The parameter  $N_i$  also represents the probability that the  $i$ th distillation step succeeds. Due to this random behavior in the generation, we have that initially the transmitter does not know which qubit is effectively useful. For this reason, it has to store them until the receiver confirms the entanglement generation (see the pictorial example in Fig. 2). As remarked in [24], the twirling performed in [23] (i.e., an operation that uniformly distributes the error states resulting in  $B = C = D$ ) has the effect to slow the convergence of  $A_i \rightarrow 1$ . For this reason, in the following, we consider the initial state to be a Werner one to show how ad hoc coding can improve this critical scenario.



In recent years, several distillation protocols have been proposed [55], [56]. However, we stick with [24] for simplicity in the analytical treatment. On the other hand, it is possible to use the proposed techniques to search for asymmetry in other distillation protocols, and then use ad hoc error correction as we will show in the following. We will touch upon the analysis of other protocols in Section IV.

## B. QUANTUM ERROR CORRECTION

We indicate with  $[[n, k, d]]$  a QECC that encodes  $k$  information qubits into a codeword of  $n$  qubits, having distance  $d$ . This code is able to correct all patterns of up to  $t = \lfloor (d-1)/2 \rfloor$  errors. We consider stabilizer codes  $\mathcal{C}$  generated by  $n-k$  independent and commuting operators  $\mathbf{G}_i \in \mathcal{G}_n$ , called generators, where  $\mathcal{G}_n$  is the Pauli group on  $n$  qubits [47], [57]. The code  $\mathcal{C}$  is the set of quantum states  $|\psi\rangle$  satisfying  $\mathbf{G}_i |\psi\rangle = |\psi\rangle$ ,  $i = 1, 2, \dots, n-k$ . These error-correcting codes preserve their information by means of measurements of extra qubits (usually referred to as ancillas), which have been properly entangled with the codeword. For the sake of clarity, assume that a codeword  $|\psi\rangle \in \mathcal{C}$  is affected by a channel error. Measuring the codeword according to the stabilizers  $\mathbf{G}_i$  with the aid of ancilla qubits, the error collapses on a discrete set of possibilities represented by combinations of Pauli operators  $\mathbf{E} \in \mathcal{G}_n$  [57]. For example, an error represented by a rotation  $\mathbf{R}_x(\theta)$  collapses into  $\mathbf{I}$  or  $\mathbf{X}$  with probability  $\cos^2(\theta/2)$  and  $\sin^2(\theta/2)$ , respectively, when the ancillae are measured according to the stabilizer. For this reason, quantum channels for stabilizer codes are described by specifying the single Pauli error probabilities. The measurement procedure over the ancilla qubits results in a quantum error syndrome  $s(\mathbf{E}) = (s_1, s_2, \dots, s_{n-k})$ , with each  $s_i = 0$  or 1 depending on  $\mathbf{E}$  commuting or anticommuting with  $\mathbf{G}_i$  [57]. A maximum likelihood decoder will then infer the most probable error  $\hat{\mathbf{E}} \in \mathcal{G}_n$  compatible with the measured syndrome. On the other hand, considering decoders correcting codewords with up to  $t = \lfloor (d-1)/2 \rfloor$  errors (i.e., the guaranteed error correction capability of a bounded distance decoder) we have that the logical qubit error probability is

$$\rho_L = 1 - \sum_{j=0}^t \binom{n}{j} \rho^j (1-\rho)^{n-j} \quad (4)$$

where  $\rho$  is the physical qubit error probability. This can be used to upper bound the error probability of the maximum likelihood decoder, while, for codes with negligible degeneracy effects, it is also a tight approximation [31]. In the following, we also consider  $[[n, k]]$  asymmetric codes able to correct up to  $e_g$  generic errors (i.e.,  $\mathbf{X}$ ,  $\mathbf{Y}$ ,  $\mathbf{Z}$ , or none) plus up to  $e_Z$  Pauli  $\mathbf{Z}$  errors, and no others [38]. In the presence of asymmetry in the error probabilities of a quantum channel, these codes can obtain improvement in performance and code length efficiency. In this setting, we define  $p_X$ ,  $p_Y$ , and  $p_Z$  as the probability to have an error of type  $\mathbf{X}$ ,  $\mathbf{Y}$ , and  $\mathbf{Z}$ , respectively. Then, by weighting each pattern with the

corresponding probability of occurrence, the expression (4) is generalized by [38]

$$\rho_L = 1 - \sum_{j=0}^{e_g+e_Z} \binom{n}{j} (1-\rho)^{n-j} \sum_{i=(j-e_g)^+}^j \binom{j}{i} p_Z^i (\rho - p_Z)^{j-i} \quad (5)$$

where  $(x)^+ = \max\{x, 0\}$  and  $\rho = p_X + p_Y + p_Z$ .

## III. AD HOC CODING OVER TELEPORTATION CHANNELS

### A. QUANTUM TELEPORTATION CHANNEL: DEFINITION

Among quantum channels, a subclass of them is described by Pauli errors, for example, due to the error collapse briefly described in Section II-B. For such channels, the qubits passing through them can experience a Pauli error  $\mathbf{X}$ ,  $\mathbf{Y}$ , and  $\mathbf{Z}$  or none. Respectively, they occur with probabilities  $p_X$ ,  $p_Y$ , and  $p_Z$ , while no errors occur with probability  $1 - \rho$ , with  $\rho = p_X + p_Y + p_Z$ . In particular, some well-known cases are represented by the following:

- 1) the bit-flip (phase-flip) channel where a qubit can experience only a  $\mathbf{X}$  ( $\mathbf{Z}$ ) error with probability  $p_X$  ( $p_Z$ );
- 2) the depolarizing channel where  $p_X = p_Y = p_Z$  [47];
- 3) the asymmetric channel characterized by asymmetry parameter  $\mathcal{A} = p_Z/p_X$ , where  $p_X = p_Y$  and  $p_Z = \mathcal{A} \rho / (\mathcal{A} + 2)$  [37], [38];
- 4) the independent  $\mathbf{XZ}$  channel where each qubit pass through a concatenation of a bit-flip and a phase-flip channel [58].

For asymmetric channels, (5) can be expressed as a function of  $\rho$  and  $\mathcal{A}$  instead of  $\rho$  and  $p_Z$ . Generally, we define the equivalent asymmetric parameter  $\mathcal{A}_{\text{eq}} = 2 p_Z / (p_X + p_Y)$ , resulting in a logical qubit error probability

$$\rho_L = 1 - \sum_{j=0}^{e_g+e_Z} \binom{n}{j} (1-\rho)^{n-j} \rho^j \left( \frac{2}{\mathcal{A}_{\text{eq}} + 2} \right)^j \times \sum_{i=(j-e_g)^+}^j \binom{j}{i} \left( \frac{\mathcal{A}_{\text{eq}}}{2} \right)^i \quad (6)$$

when asymmetric codes are adopted. On the other hand, symmetric codes whose performance is described by (4) are not affected by any error imbalance since they act on generic errors. Since the asymmetric channel is a particular case of the defined equivalent asymmetric channel, in the following, we use the  $\mathcal{A}_{\text{eq}}$  parameter dropping the notation equivalent for the sake of simplicity.

Due to imperfections in EPR pairs, the quantum teleportation protocol can be interpreted as a quantum communication channel [23]. In fact, considering an information state  $|\psi\rangle$  to be teleported and the EPR pair  $|\Psi^+\rangle$  instead of  $|\Phi^+\rangle$  as described in Section II, at the end of the teleportation algorithm we obtain  $\mathbf{X} |\psi\rangle$ . In general, considering a mixture of EPR pairs as in (1), we can describe the quantum teleportation with a surrogate channel having  $p_X = C$ ,  $p_Y = B$ , and  $p_Z = D$  (see Fig. 3). We point out that in particular, assuming

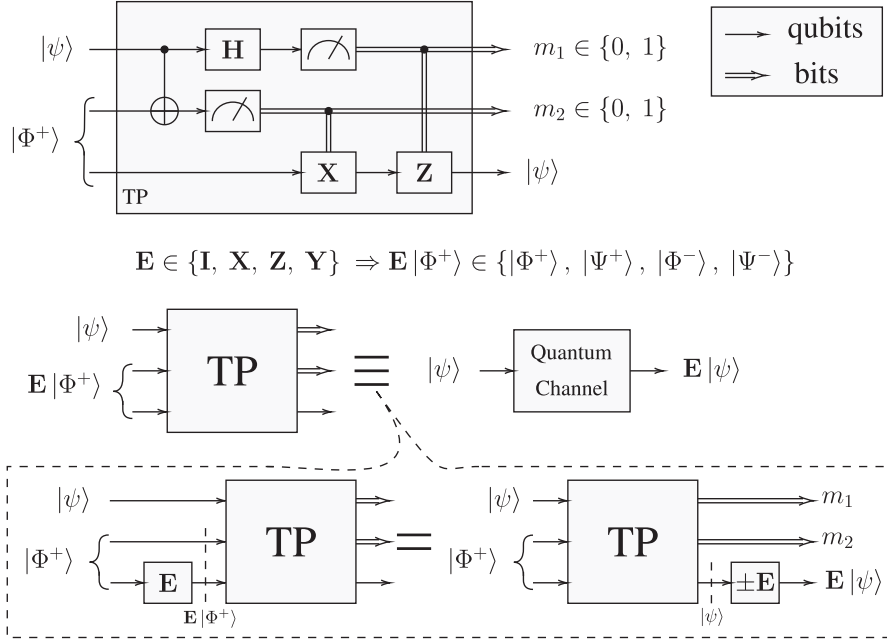


**FIGURE 3.** Equivalence between teleportation protocol using noisy EPR pair and a quantum communication channel based on Pauli errors.

a Werner state as the shared pair, teleportation is equivalent to transmission over a depolarizing channel.

This observation, despite its simplicity, is the bridge to connect quantum distillation and QEC in the direction of reliable low-latency communications, adaptive QEC for quantum networks, and mid-generation error management schemes.

### B. QUANTUM TELEPORTATION CHANNELS: ANALYSIS

In this section, we report an analysis of the distillation protocol proposed in [24], described in Section II-A. Our aim is to show that distillation protocols tends to generate asymmetries in the output entangled pair, which can be exploited by asymmetric error correction schemes. In particular, we consider shared pairs in the Werner state (2) with an initial fidelity  $\mathcal{F}_0$ . The following analysis can be conducted to search for asymmetries in other distillation protocols or under different initial conditions. Yet, the analytical treatment could not be always feasible.

In our setting, we have that after one step of distillation the state evolves into

$$\begin{aligned}
 A_1 &\propto \mathcal{F}_0^2 + (1 - \mathcal{F}_0)^2/9 \\
 B_1 &\propto 2(1 - \mathcal{F}_0)^2/9 \\
 C_1 &\propto 2(1 - \mathcal{F}_0)^2/9 \\
 D_1 &\propto 2\mathcal{F}_0(1 - \mathcal{F}_0)/3
 \end{aligned} \quad (7)$$

where we have omitted the common normalization factor. We observe that the equivalent quantum teleportation channel evolved from the depolarizing channel to the asymmetric channel is described in Section III-A. To describe such a channel it is sufficient to give the error probability  $\rho$  and the

equivalent asymmetry parameter  $\mathcal{A}_{\text{eq}}$ . In our case, we have

$$\mathcal{A}_{\text{eq},1} \triangleq \frac{2D_1}{B_1 + C_1} = 3 \left( \frac{1}{\rho_0} - 1 \right) \quad (8)$$

$$\rho_1 \triangleq B_1 + C_1 + D_1 = 2\rho_0 \frac{3 - \rho_0}{9 - 12\rho_0 + 8\rho_0^2} \quad (9)$$

where  $\rho_0 = 1 - \mathcal{F}_0$  is the initial error probability. From (9), we note that, even considering  $\rho_0 \ll 1$ , the error probability tends to  $2\rho_0/3$ . This limited improvement is the cause of the algorithm in [23] requiring more distillation steps than [24] in order to acquire the same target fidelity. Considering symmetric QEC, the improvement given by one step of distillation is likely not worth it compared with the cost in raw EPR pairs. However, in asymmetric QEC, the performance is affected both by the error and asymmetry parameters, making them appealing for this scenario. In fact, in (8), we can observe the effectiveness of the first step of distillation in increasing the asymmetry of the channel from  $\mathcal{A}_{\text{eq}} = 1$  to  $\mathcal{A}_{\text{eq}} \approx 3/\rho_0$ .

In Fig. 4, we report the state evolution of the EPR pairs distilled by (3) and assuming to start from the Werner state with  $\mathcal{F}_0 = 0.8$ . As shown in (7), and as depicted in Fig. 4, the quantum teleportation channel after one step of distillation becomes asymmetric in the conventional sense (i.e.,  $p_X = p_Y$ ). More in general, this happens whenever the previous state has  $C_{i-1} = D_{i-1}$ . In fact, having a state with parameter  $\{A, B, C, D\}$  equal to  $\{A, B, k, k\}$ , by applying (3), we end up to a state with  $\{A^2 + B^2, 2k^2, 2k^2, 2AB\}$ , where the common normalization factor has been omitted. Observing the distillation procedure only between  $i = 0$  and  $i = 4$ , it seems that having an asymmetric channel at step  $i$  provides a state with  $C_{i+1} = D_{i+1}$  at step  $i + 1$ . However, this is not true in general as has been reported in the plot evolving the

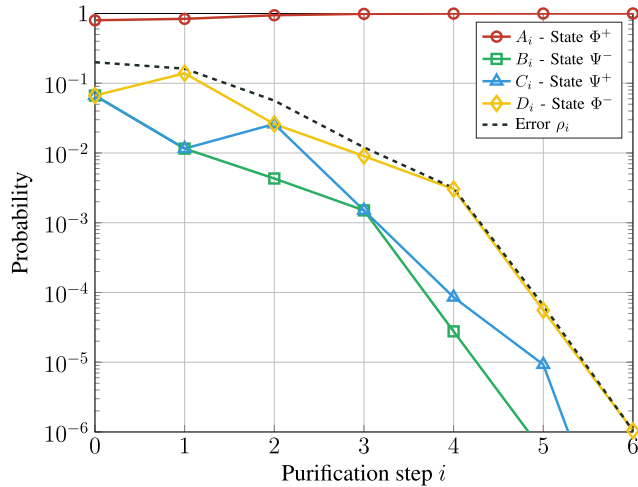


**FIGURE 4.** Evolution of the probability distribution of the EPR pairs' mixture described by (1) due to distillation algorithm (3). The initial state is a Werner state with fidelity  $\mathcal{F}_0 = 0.8$ .

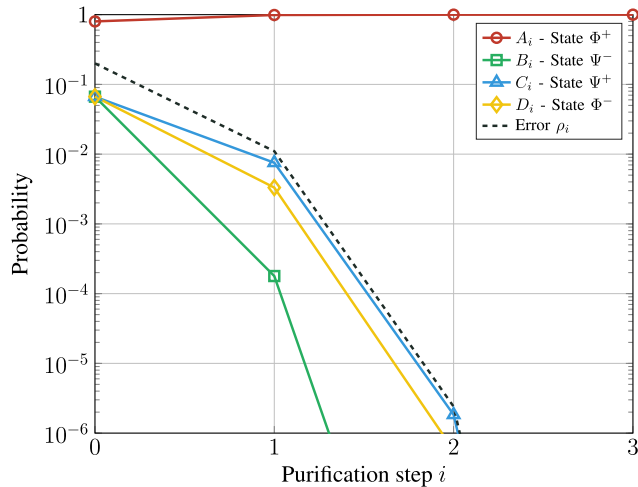


**FIGURE 5.** Evolution of the probability distribution of the EPR pairs' mixture described by (1) due to the STRINGENT distillation algorithm [59]. The initial state is a Werner state with fidelity  $\mathcal{F}_0 = 0.8$ .

state from step  $i = 3$  to  $i = 4$  [or by checking (3)]. The fact that we have  $C_2 = D_2$  is a consequence of the Werner state assumption  $B_0 = C_0 = D_0$  and not due to  $B_1 = C_1$ . Noted that this initial behavior is not recursive we observe that the teleportation channel tends to be asymmetric in the sense that  $D_i \gg B_i + C_i$  for  $i > i_{\min}$ , where  $i_{\min}$  depends on the initial fidelity  $1 - \rho_0$ . We conclude that asymmetries arise in the distilled pairs. Hence, exploiting this feature of distillation protocols could play a key role to improve the performance of quantum communication.

As a comparison to newer distillation protocols, we show in Fig. 5 the same setup as in Fig. 4, but using the STRINGENT protocol [59] rather than the Deutsch et al. [24] distillation in (3). While we do see a larger improvement in fidelity in each step, one should note that the STRINGENT circuit is more complicated and requires a large amount of gates and measurements compared with the distillation in (3).

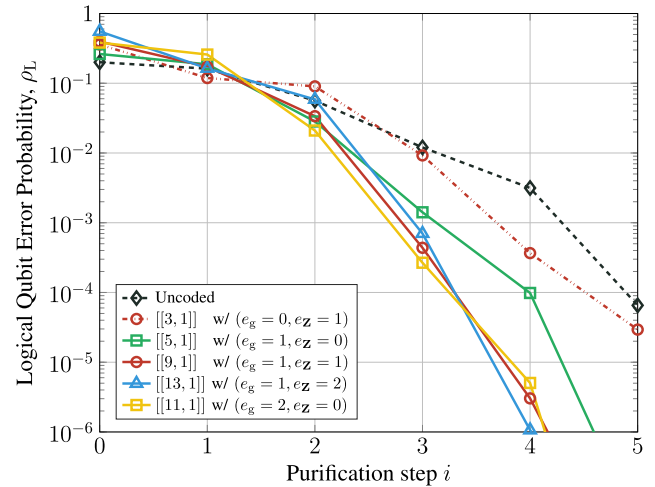


**FIGURE 6.** Logical qubit error probability as a function of distillation steps for different coding schemes. We consider bounded distance decoding for  $[[n, k]]$  codes with  $(e_g, e_z)$  error correction capability as reported in (6). The initial state is a Werner one with fidelity  $\mathcal{F}_0 = 0.8$ .

This also shows in the success probabilities. For the initial fidelity  $\mathcal{F}_0 = 0.8$  considered here, the first step of distillation using STRINGENT has  $\sim 5.8\%$  success probability, while increasing the fidelity to  $\sim 0.99$ . On the other hand, the three first steps of the older distillation protocol by Deutsch et al. [24] have a combined success probability of  $\sim 51.6\%$  while still delivering a fidelity of  $\sim 0.99$ . Clearly, a lower success probability implies that more distillation attempts are necessary to obtain the same number of distilled pairs. Thus, one needs to either perform more distillations in parallel (increasing the requirements on quantum memory and processing power), or more distillations sequentially (increasing the latency). Neither option is desirable in our setting, for which reason we will restrict ourselves to the distillation procedure summarized in (3).

Ad hoc QEC represents one possible way to exploit the particular channel configurations, which are evolving due to distillation. To this aim, we report in Fig. 6 the performance, in terms of logical error probability (i.e., one minus the reliability), of some  $[[n, k]]$  codes with  $(e_g, e_z)$  error correction capability, varying the number of distillation steps  $i$ . In general, for codes with  $e_g > 0$ , we have that after a distillation step  $\ell$ , the coded scheme starts to outperform the uncoded one and it continues to outperform the uncoded for each  $i > \ell$ . In particular,  $\ell$  depends on the code and the initial error probability  $\rho_0$ , which is fixed to  $\rho_0 = 0.2$  in the plot. Reading the plot horizontally, it is also possible to obtain some insights in terms of latency. In fact, when targeting a reliability  $1 - \rho_L^*$ , we have that the uncoded scheme requires more distillation steps, which is in some situations equivalent to saying that it requires more classical protocol messages. Finally, we want to emphasize that, observing only the symmetric codes, we have that larger codes are always better after a certain threshold  $\ell$ . In other words, after a certain threshold, there is an order on the  $\rho_L$  of the codes, which is preserved,

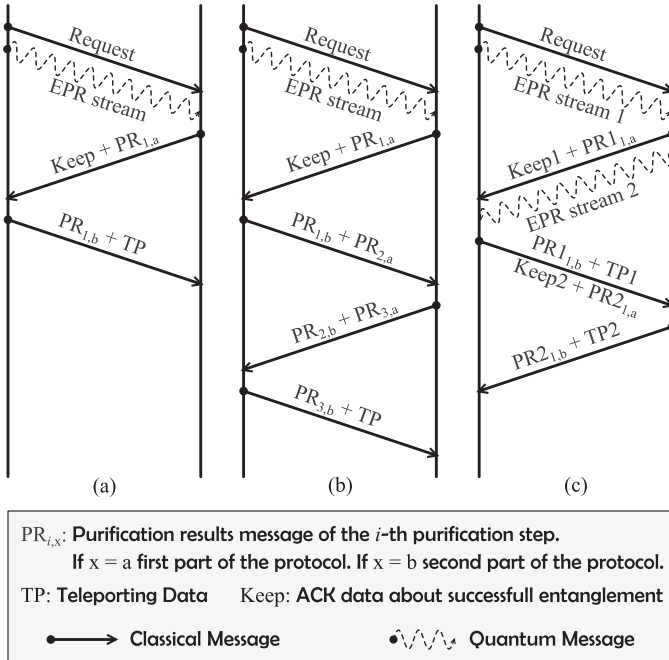


**FIGURE 7.** Protocol messaging for EPR pair creation, distillation, and teleportation. Message exchange for: (a) single distillation, (b) three distillations, and (c) back-and-forward protocol with single distillation.

due to the fact that the distillation protocol converges to fidelity one [54], and larger codes have larger  $e_g$ . On the other hand, when asymmetric codes are considered, the channel asymmetry  $\mathcal{A}_{eq,i}$  becomes an important design parameter alongside  $\rho_i$ . Hence, the code must be chosen carefully depending on the particular quantum teleportation channel.

### C. LOW-LATENCY PROTOCOLS: SINGLE QUANTUM LINK

In this section, we address on-demand single quantum link teleportation protocols having low-latency constraints. In particular, we aim at minimizing the number of message exchanges necessary to establish reliable communication. Let us begin with a forward communication protocol between two nodes.

As discussed in [26] and illustrated in Fig. 7(a), it is possible to create a quantum channel by the means of distilled EPRs (one distillation step) with a three steps procedure. First, the node that desires to communicate something generates  $M$  EPR pairs and sends a request message followed by the qubits for entanglement distribution among the two nodes [17], [18], [19], [20], [21]. This heralded entanglement generation is classified as “at source” generation [11], [60]. The receiver, if not busy, stores into its quantum memory the qubits whose entanglement is guaranteed by a detector [17], [61]. Then, it performs the local operations required for the first step of distillation as reported in Section II-A. Defining  $p$  as the probability to receive a qubit and that it is correctly entangled, the number of received qubits  $n_0$  is distributed according to a binomial distribution with  $M$  trials and success probability  $p$  (sometimes also referred to as the emission probability).

Second, it transmits the information regarding which initial EPR pair has been successfully received (usually referred to as a *keep* message), which pairs have been selected for distillation, and its partial distillation results obtained by the measurement step. Upon receiving this information, the user who initially asks for the channel can apply the distillation procedure on the appropriate pairs and based on the results understand which pair have been successfully distilled. At this point, the number of EPR pairs  $n_1$  after one step of distillation is given again by a binomial distribution with  $\lfloor n_0/2 \rfloor$  trials and success probability  $N_1 = (A_1 + B_1)^2 + (C_1 + D_1)^2$  due to the distillation described in (3). Referring to the example, as shown in Fig. 2, we have that starting with  $M = 13$  pairs, the receiver detects  $n_0 = 7$  qubits, and at the end of one distillation step, we end up with  $n_1 = 2$  distilled EPR pairs.

Lastly, the user can either concatenate another distillation step, concatenate the quantum information teleportation, or simply end the distillation, sending the measurement results.

To nest a second distillation step, the transmitter has to repeat the same operations performed by the receiver at step two. Consequently, it appends to the first distillation measurement data (which act as a *keep* message at this point), the new measurements, and corollary information. As an example, we report in Fig. 7(b) a protocol with three nested distillations. Due to the fact that we are targeting low-latency protocols, we consider directly teleporting quantum data. This also represents the protocol with the lowest latency since entanglement generation is a sporadic event, making the *keep* message mandatory. To be precise, without EPR pair confirmation, the link fidelity would be lower bounded by entanglement generation probability (usually very low for long-distance generation), which is reflected in an unusable link. Hence, transmitting this *keep* message, one distillation step can always be performed without any significant cost in latency.

To increase the fidelity, we propose a hybrid scheme using both distillation and QEC. In fact, instead of using the teleportation protocol on the quantum data, it is possible to teleport a quantum codeword that represents the encoded data. As usual, applying QEC we aim to improve the reliability of the system at the cost of transmission rate. In particular, adopting an  $[[n, k]]$  code we need  $n$  EPR pairs to teleport  $k$  information qubit. Since in mid-generation it could be difficult to construct long and complex QECCs, which are the target for third-generation error management schemes [11], in the following, we consider short codes [34], [35], [38], [62].

In (8), we have observed that starting from a Werner state, we gain asymmetry in the equivalent quantum channel after one distillation step. Taking this into account, as shown by the generalized quantum Hamming bound [38], we can design ad hoc codes, which either use fewer qubits to achieve the same performance or vice versa. In this asymmetric scenario, also very simple codes, such as the  $[[n, 1]]$  with  $e_g = 0$  and  $e_z = \lfloor n/2 \rfloor$  (i.e., repetition codes), can be of practical interest. This is motivated by the encoder and decoder



simplicity and the performance boost they can provide in the presence of strong asymmetry. More generally, adopting  $[[n, k]]$  with error correction capability ( $e_g, e_z$ ) in this hybrid communication protocol, we will show in Section IV the overall achievable fidelity improvements.

Finally, we discuss the possibility to have a reliable back-and-forward communication protocol. This protocol, depicted in Fig. 7(c), is intended for applications in which a node has to send a qubit to a neighbor for multiqubit processing. This operation (e.g., a CNOT) is performed between the neighbor qubits and the sent qubit, consequently, it is sent back to its owner. Some application examples are represented by multicore quantum computing [6], construction of quantum graph state [43], [44], [45] over networks, and in general, all applications where it is useful to extend the concept of local operations to neighbors. In comparison with the conventional protocol in Fig. 7(a) having only the *forward-link* created using the first EPR stream, during the second transmission, a second EPR stream is concatenated to create the *back-link*. As usual, after three transmissions, the receiver holds the transmitter qubit and can perform its processing. When the processing is done, using the *back-link*, it is possible to send back the qubit with just one classical transmission. Increasing the stream size and the initial quantum memory  $M$  accordingly, it is possible to parallelize this procedure to transmit a packet of qubits. This can be done using  $[[n, k]]$  codewords with  $k > 1$  or concatenation of  $[[n, 1]]$  codewords.

*Note:* A double-size quantum memory is not required for this link communication. This is due to the fact that the receiver can allocate its new EPR pair qubits (EPR stream 2) in memories that have nongenerated entangled pairs, measured qubits, and discarded qubits. For example, in Fig. 2, EPR stream 1 is composed of 13 qubits, while EPR stream 2 might be composed by up to ten qubits. For this reason, the initial memory  $M$  may increase, but it is not necessary to double it.

#### D. LOW-LATENCY PROTOCOLS: QUANTUM NETWORKS

The entanglement distribution over quantum networks is achieved using the entanglement swapping protocol [11]. This protocol is the conventional quantum teleportation which, instead of transmitting one qubit of information, transmits one qubit of an entangled pair [63]. For the sake of clarity, let us consider this example. Three users  $u_1, u_2$ , and  $u_3$  share two EPR pairs  $|\Phi^+\rangle_{12}$  and  $|\Phi^+\rangle_{23}$ , where the subscripts indicate which users have the qubits. User 2 can teleport its qubit of the pair  $|\Phi^+\rangle_{12}$  to  $u_3$  using  $|\Phi^+\rangle_{23}$  as described in Section II resulting in a single pair with state  $|\Phi^+\rangle_{13}$ . An example of this entanglement swapping protocol [26], [52], [63] with nine nodes (i.e., eight hops) is depicted in Fig. 8.

In general, this protocol deteriorates the quality of the entangled pair. To be precise, taking into account the same probability distributions for the pair used to teleport and for the pair in which one qubit has been teleported, we obtain a probability evolution of the characteristic parameters

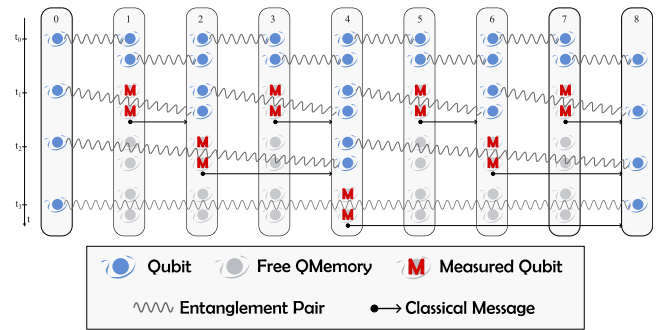


**FIGURE 8.** Nested entanglement swapping procedure to share EPR pairs between far away nodes. In the example, we have a network with eight hops, which requires three swapping steps.

described by

$$\begin{aligned} A_{i+1} &= A_i^2 + B_i^2 + C_i^2 + D_i^2 \\ B_{i+1} &= 2A_iB_i + 2C_iD_i \\ C_{i+1} &= 2A_iC_i + 2B_iD_i \\ D_{i+1} &= 2A_iD_i + 2C_iB_i \end{aligned} \quad (10)$$

where again  $i$  represents the current step since the initial probability distribution in (1) evolves according to (3) or (10). It is important to note that, after  $\ell$  swapping steps, we are able to cover  $2^\ell$  link hops.

According to (10), the protocol tends to the stable and equiprobable configuration  $A_i = B_i = C_i = D_i$ . Hence, the distillation protocol has to compensate also for this fidelity loss in order to guarantee the target fidelity. For this reason, we propose a protocol name Burst  $b$ , where  $b$  is the number of distillation steps done. In this protocol, we first schedule  $b$  single-link distillations [e.g., Burst 1 in Fig. 7(a) and Burst 3 in Fig. 7(b)]. Consequently, we perform the necessary entanglement swap over these distilled pairs. This protocol has the advantage that it significantly reduces the control signaling in the network since it uses only single-link distillation. In other words, it improves the latency of the communication. Moreover, it snowballs the fidelity improvement given by distillation before letting the swapping protocol degrade the fidelity. This has the advantage to improve also the reliability compared with the protocol stack proposed in [26] where distillation and swapping are alternated in order to keep the fidelity above the target. We performed extensive numerical investigations for several initial quantum states and, based on the results, we conjecture that the proposed approach is the optimal scheduling. A formal proof of optimality, which seems nontrivial, is left as a future work.

Similarly to single-link quantum communication protocols, we can adopt QEC to construct a hybrid scheme capable of reliably transmitting the quantum information. From (10), we observe that for small error probability (i.e.,  $\rho_i \ll 1$ ) and nontrivial unbalance in the particular error probabilities, we have that  $B_{i+1} \approx 2B_i$ ,  $C_{i+1} \approx 2C_i$ , and  $D_{i+1} \approx 2D_i$ . Then, we can state that entanglement swapping preserves the asymmetries of the equivalent quantum channel. As a consequence,

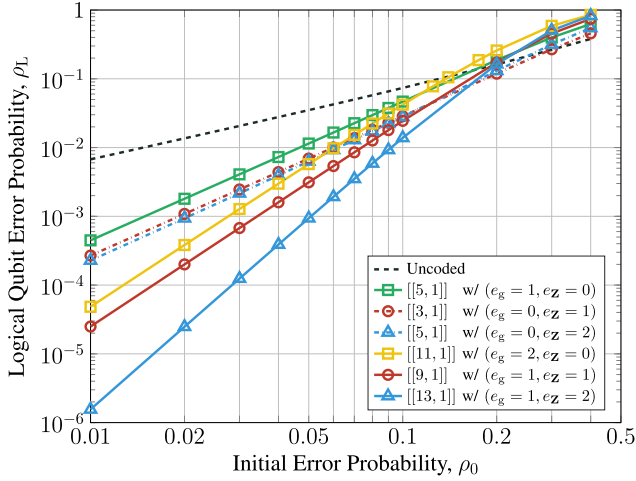


**FIGURE 9. Logical qubit error probability against the initial error probability  $\rho_0 = 1 - \mathcal{F}_0$  considering a single distillation step. We consider bounded distance decoding for  $[[n, k]]$  codes with  $(e_g, e_z)$  error correction capability as reported in (6).**

for practical consideration, the asymmetry  $\mathcal{A}_{\text{eq},i}$  is given by the initial state and the number of distillation steps. For this reason, the entanglement swapping protocol affects the QEC code design only by deteriorating the error parameter  $\rho_i$ .

#### IV. NUMERICAL RESULTS

In this section, we report the performance comparison of quantum hybrid communication protocols, using the logical qubit error probability  $\rho_L$ , as given in (6). To evaluate the parameter of (6), we first use (3) and (10) to find the final distilled pair state  $\{A, B, C, D\}$ , and then, we find  $\mathcal{A}_{\text{eq}} = 2D/(B+C)$  and  $\rho = B+C+D$ . In this way, we do not require Monte Carlo simulation to evaluate the results. We report these comparisons for both the single-link and network scenarios, varying the adopted  $[[n, k]]$  with  $(e_g, e_z)$  error correcting code. Due to implementation reasons, we focus our results on short quantum codes, such as the  $[[3,1]]$  and  $[[5,1]]$  repetition codes, the five-qubit code [35], the  $[[11,1]]$  code able to correct up to two generic errors [36], and the  $[[9,1]]$  and  $[[13,1]]$  asymmetric codes [38]. In the following, we consider only the case where the initial state is a Werner one.

##### A. AD HOC CODING OVER SINGLE QUANTUM LINK

In Fig. 9, we report the performance of a low-latency single quantum link communication varying the initial error probability  $\rho_0$ , where a single step of distillation is performed [see Fig. 7(a)]. The uncoded curve shows again that one distillation step does not significantly improve the fidelity when starting from a Werner state. However, this apparently useless step is able to give us an asymmetry, we can exploit by ad hoc coding. In fact, adopting asymmetric QECCs (i.e.,  $e_z > 0$ ), we obtain an important performance boost. From the plot, we can observe some interesting behaviors. First, we note that the simple and easy-to-implement  $[[3,1]]$  repetition code for a phase-flip channel can outperform the five-qubit code ( $e_g = 1$ ). In fact, in the presence of strong

asymmetry, these two codes have the same effective error correction capability. Hence, the one with fewer qubits is able to outperform the other both in terms of error probability and codeword length. Second, considering the  $[[5,1]]$  repetition code, we observe no improvement compared with the  $[[3,1]]$ . This is due to the fact that the double  $Z$  error is approaching the same occurrence probability of a single  $X$ , which is limiting further improvement. Similarly, the performance comparison between the  $[[11,1]]$  and  $[[9,1]]$  codes shows that it is inefficient to protect against generic errors when the asymmetry is sufficiently large. Third, we note that, for a fixed  $e_g$ , we obtain an improvement by increasing  $e_z$ , as it is shown for the  $[[9,1]]$  and  $[[13,1]]$  asymmetric codes. This is not an obvious result, since to increase  $e_z$ , we have to increase the codeword length, making the overall performance depending also on the channel asymmetry. In the case of Fig. 9, the channel asymmetry makes it advantageous to use codes with larger correction capability against  $Z$  errors. Finally, considering a target logical qubit error probability  $\rho_L^* = 10^{-3}$ , while without codes, we need an initial fidelity  $\mathcal{F}_0 \geq 99.85\%$ , using the  $[[3,1]]$  repetition code, we require an initial fidelity  $\mathcal{F}_0 \geq 98\%$ , and with the  $[[13,1]]$  asymmetric code, we require an initial fidelity  $\mathcal{F}_0 \geq 95\%$ .

Another way to use Fig. 9 is to perform code selection. Given the link parameter  $\{A, B, C, D\}$  and a number of available distilled pairs, using (6), we can find the code with lowest  $\rho_L$  using at most the number of available pairs. Since the results are analytically derived, this does not require simulations. This analysis can be extended also to topological codes using minimum weight perfect matching decoders since analytical logical error rates was recently derived in [32]. Adopting other distillation algorithms, e.g., STRINGENT, it is possible to perform the same analysis numerically evaluating the corresponding  $\rho_i$  and  $\mathcal{A}_{\text{eq},i}$  of those protocols as a function of  $\rho_0$ . Then, using (6) for each desired code, one can obtain a performance comparison similar to the one in Fig. 9. Whether an improvement is seen depends on the  $\rho_i$  and  $\mathcal{A}_{\text{eq},i}$  of the specific distillation algorithm.

##### B. QUANTUM NETWORK ANALYSIS

In Fig. 10, we report the effect on the qubit error probability  $\rho_i$  in a quantum network scenario, varying the number of swapping steps  $i$  and considering the Burst  $b$  protocols proposed in Section III-D. As expected, when  $\rho_1$  is sufficiently small we have that  $\rho_i \approx 2^{i-1} \rho_1$ . Then, to design an uncoded scheme, it is sufficient to fix an  $i_{\text{max}}$  of steps we need to cover and act on  $b$  in order to satisfy  $\rho_L^* \geq 2^{i_{\text{max}}-1} \rho_1$ . Note that the number of swapping steps is not the number of link hops. To be precise, we can cover  $2^i$  hops with  $i$  swapping step (see Fig. 8). From the plot, we point out that Burst 1 schemes, and in general, all network schemes with just one distillation step, always give  $\rho_i > \rho_0$ ,  $i \geq 1$ . This is because one distillation step gives a  $2/3$  improvement factor, while the swapping gives a factor 2 degradation, resulting, for nontrivial Werner states with  $\rho_0 < 0.75$ , in  $\rho_1 \approx 4\rho_0/3$  for low  $\rho_0$ . Then, to gain an improvement in the qubit error

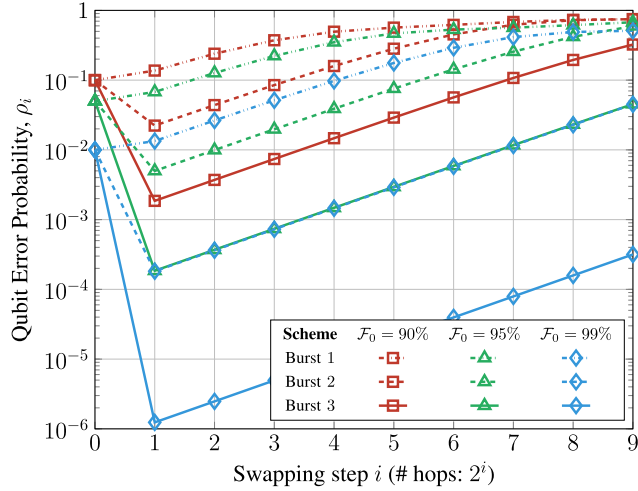


**FIGURE 10.** Evolution of the equivalent quantum teleportation channel error probability  $\rho_i$  due to entanglement swapping (10), for burst  $b = 1, 2, 3$  protocols and initial fidelity  $\mathcal{F}_0 = 90\%, 95\%, 99\%$ .

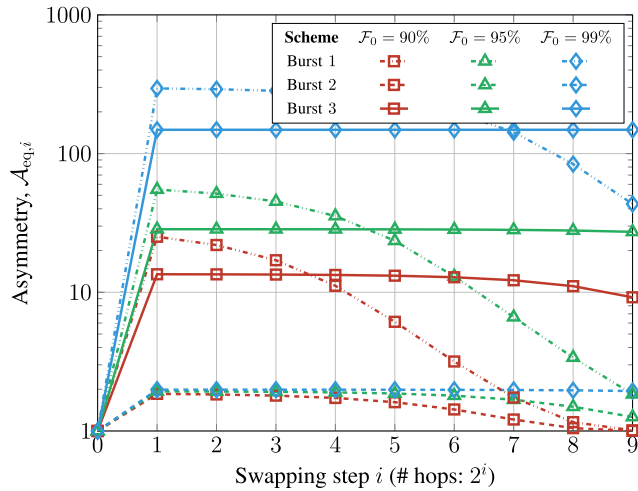


**FIGURE 11.** Evolution of the quantum teleportation channel equivalent asymmetry  $\mathcal{A}_{eq,i}$  due to entanglement swapping (10), for burst  $b = 1, 2, 3$  protocols and initial fidelity  $\mathcal{F}_0 = 90\%, 95\%, 99\%$ . The asymmetry  $\mathcal{A}_{eq} = 1$  represents the well-known depolarizing channel.

probability, we have to adopt Burst  $b$  schemes with  $b > 1$ . For example, considering an initial fidelity  $\mathcal{F}_0 = 90\%$ , we have  $\rho_i < \rho_0$  until swapping step 3 and step 6 for Burst 2 and Burst 3 protocols.

In Fig. 11, we report the effect on the equivalent asymmetry  $\mathcal{A}_{eq,i}$  in a quantum network scenario, varying the number of swapping steps  $i$  for Burst  $b$  protocols. As expected from Fig. 4, we have that Burst 1 and Burst 3 give good asymmetry values for ad hoc coding, while Burst 2 is almost symmetric ( $p_Z = p_X$  as can be observed from Fig. 4). For this reason, even if Burst 2 can already provide  $\rho_i < \rho_0$  for some values of  $i$ , it can be useful to use Burst 3 aiming to adopt ad hoc QEC over the distilled pairs. Moreover, we remind that in terms of latency, Burst 2 and Burst 3 are equivalent, as shown in Fig. 7(b). As previously discussed in Section III-D, for  $\rho_i$  of practical interest (i.e.,  $\rho_i < 0.1$ ), we can see that the asymmetry is preserved when the swapping protocol is performed.

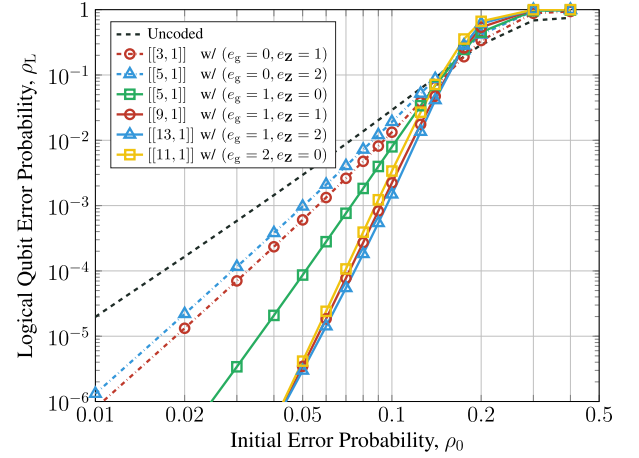


**FIGURE 12.** Logical qubit error probability against the initial error probability  $\rho_0 = 1 - \mathcal{F}_0$  considering the Burst 3 protocol and five swapping steps (i.e., 32 network hops). We consider bounded distance decoding for  $[[n, k]]$  codes with  $(e_g, e_z)$  error correction capability as reported in (6).

### C. AD HOC CODING OVER QUANTUM NETWORK

In Fig. 12, we report the performance of communication over a quantum network by varying the initial error probability  $\rho_0$ , where Burst 3 is adopted and five swapping steps are performed. Regarding the comparison with Fig. 9, in this case, QECCs act on a different regime. In fact, comparing channel parameters for 1 and 3 steps of distillation, we have that the asymmetries  $\mathcal{A}_{eq,i}$  are similar (see also Fig. 11), but the error probabilities  $\rho_i$  are much smaller when accounting for three distillation steps. For this reason, the symmetric five-qubit code outperforms the repetition codes designed for phase-flip errors. Larger codes with  $n \geq 9$  give further improvements, as reported in the figure. More precisely, since the channel is asymmetric, we can suitably design asymmetric codes, balancing  $e_g$  and  $e_z$ . This can be easily seen from the plot, observing that the  $[[11, 1]]$  symmetric code performs practically the same as the  $[[9, 1]]$  asymmetric code. The latter code, requiring fewer qubits per codeword, could be thus preferred for practical implementations. In general, we emphasize that an estimation of the initial parameters can be exploited for a tailored QECC design. These parameters could be taken from the nominal one given by the adopted technology. However, when these parameters are not available, asymmetry cannot be exploited and the only possibility to reduce the protocol latency, compared with distillation-only schemes, is to construct suboptimal hybrid schemes using symmetric QECCs.

### V. DISCUSSION AND FUTURE WORKS

In this work, our focus has lied on low-latency protocols, demonstrating that good performance can also be achieved when few steps of distillation are considered. In the current vision, first generation networks will adopt only distillation to make the communication reliable, while third generation networks will adopt only QEC to have both reliable and low-latency communication protocols [11], [42]. In our



envisioned trajectory, positioned between these two generations, hybrid schemes could emerge, leveraging distillation while also addressing latency concerns.

One possible direction for future works could deepen the discussion on the advantages of combining distillation and QEC instead of directly distilling perfect EPR pairs. Such an exploration could provide valuable insights into the conditions under which quantum networks can attain sufficient reliability, thereby enabling a shift from addressing solely reliability through distillation to addressing broader concerns (e.g., latency), marking the transition from first-generation to second-generation networks. This can be done by conducting a comparative analysis across schemes employing varying numbers of distillation steps. In addition to the provided framework, to have a comprehensive analysis for protocols with different latency, it is necessary to take into account that the scheme with the larger latency will hold the following:

- 1) suffer more decoherence;
- 2) keep the communication link busy for more time;
- 3) slow down the applications requiring the teleportation.

Another possible direction is the assessment of the asymmetry, a crucial aspect in order to choose a proper coding strategy. Quantum communication links could be: 1) non-adaptive and 2) adaptive. In nonadaptive quantum communication links, we can choose a proper coding scheme based on the adopted technology for distributing entanglement. In fact, given the technology, we have the initial state probability distribution  $\{A_0, B_0, C_0, D_0\}$ . Having a fidelity target (or equivalently a reliability target), we can therefore execute our analysis to find the final asymmetry and the best solution. In adaptive quantum communication links, we could imagine a protocol that periodically estimates  $\{A_0, B_0, C_0, D_0\}$  (e.g., via tomography), and then adapts the coding scheme, accordingly.

## VI. CONCLUSION

We proposed hybrid schemes where distillation is used together with asymmetric QECCs to exchange information over a quantum network. The key idea is that distillation gives rise to an equivalent quantum communication channel with asymmetric Pauli error probabilities. We show that significant performance improvements can be achieved by performing a few steps of distillations, followed by teleporting protected with QECCs. For example, starting from a Werner state, assuming one distillation step and a target logical qubit error probability  $10^{-3}$ , the distillation-only protocol requires an initial fidelity  $\mathcal{F}_0 \geq 99.85\%$ , while the proposed hybrid protocol using an asymmetric  $[[13,1]]$  code works with  $\mathcal{F}_0 \geq 95\%$ . In a quantum network scenario where several swapping steps are needed to connect two nodes, we have shown how to design efficient hybrid schemes fulfilling given network quality requirements. It results that, for both single-link and quantum network scenarios, the proposed hybrid distillation/QEC protocols give substantial advantages in terms of latency and fidelity with respect to distillation-only communication protocols.

## REFERENCES

- [1] S. Wehner, D. Elkouss, and R. Hanson, "Quantum Internet: A vision for the road ahead," *Science*, vol. 362, no. 6412, 2018, Art. no. eaam9288, doi: [10.1126/science.aam9288](https://doi.org/10.1126/science.aam9288).
- [2] A. S. Cacciapuoti, M. Caleffi, F. Tafuri, F. S. Cataliotti, S. Gherardini, and G. Bianchi, "Quantum Internet: Networking challenges in distributed quantum computing," *IEEE Netw.*, vol. 34, no. 1, pp. 137–143, Jan./Feb. 2020, doi: [10.1109/MNET.001.1900092](https://doi.org/10.1109/MNET.001.1900092).
- [3] M. Pompili et al., "Experimental demonstration of entanglement delivery using a quantum network stack," *npj Quantum Inf.*, vol. 8, no. 1, 2022, Art. no. 121, doi: [10.1038/s41534-022-00631-2](https://doi.org/10.1038/s41534-022-00631-2).
- [4] C. H. Bennett and G. Brassard, "Quantum cryptography: Public key distribution and coin tossing," *Theor. Comput. Sci.*, vol. 560, pp. 7–11, 2014, doi: [10.1016/j.tcs.2014.05.025](https://doi.org/10.1016/j.tcs.2014.05.025).
- [5] C. H. Bennett and S. J. Wiesner, "Communication via one- and two-particle operators on Einstein-Podolsky-Rosen states," *Phys. Rev. Lett.*, vol. 69, no. 20, 1992, Art. no. 2881, doi: [10.1103/PhysRevLett.69.2881](https://doi.org/10.1103/PhysRevLett.69.2881).
- [6] H. Jnane, B. Undseth, Z. Cai, S. C. Benjamin, and B. Koczor, "Multicore quantum computing," *Phys. Rev. Appl.*, vol. 18, no. 4, 2022, Art. no. 044064, doi: [10.1103/PhysRevApplied.18.044064](https://doi.org/10.1103/PhysRevApplied.18.044064).
- [7] R. G. Sundaram, H. Gupta, and C. Ramakrishnan, "Distribution of quantum circuits over general quantum networks," in *Proc. IEEE Int. Conf. Quantum Comput. Eng.*, 2022, pp. 415–425, doi: [10.1109/QCE53715.2022.00063](https://doi.org/10.1109/QCE53715.2022.00063).
- [8] D. Ferrari, S. Carretta, and M. Amoretti, "A modular quantum compilation framework for distributed quantum computing," *IEEE Trans. Quantum Eng.*, vol. 4, pp. 1–13, 2023, doi: [10.1109/TQE.2023.3303935](https://doi.org/10.1109/TQE.2023.3303935).
- [9] C. L. Degen, F. Reinhard, and P. Cappellaro, "Quantum sensing," *Rev. Modern Phys.*, vol. 89, no. 3, 2017, Art. no. 035002, doi: [10.1103/RevModPhys.89.035002](https://doi.org/10.1103/RevModPhys.89.035002).
- [10] S. Bi, "Research on quantum remote sensing science and technology," in *Proc. Infrared Remote Sens. Instrum. XXVII*, 2019, pp. 167–186, doi: [10.1117/12.2528305](https://doi.org/10.1117/12.2528305).
- [11] W. Kozłowski et al., "Architectural principles for a quantum internet," RFC Editor, RFC 9340 Mar. 2023, doi: [10.17487/RFC9340](https://doi.org/10.17487/RFC9340).
- [12] C. H. Bennett, G. Brassard, C. Crépeau, R. Jozsa, A. Peres, and W. K. Wootters, "Teleporting an unknown quantum state via dual classical and Einstein-Podolsky-Rosen channels," *Phys. Rev. Lett.*, vol. 70, no. 13, 1993, Art. no. 1895, doi: [10.1103/PhysRevLett.70.1895](https://doi.org/10.1103/PhysRevLett.70.1895).
- [13] A. G. Fowler, D. S. Wang, C. D. Hill, T. D. Ladd, R. V. Meter, and L. C. Hollenberg, "Surface code quantum communication," *Phys. Rev. Lett.*, vol. 104, no. 18, 2010, Art. no. 180503, doi: [10.1103/PhysRevLett.104.180503](https://doi.org/10.1103/PhysRevLett.104.180503).
- [14] D. M. Greenberger, M. A. Horne, and A. Zeilinger, "Going beyond Bell's theorem," in *Bell's Theorem, Quantum Theory and Conceptions of the Universe*. 1989, pp. 69–72, doi: [10.1007/978-94-017-0849-4](https://doi.org/10.1007/978-94-017-0849-4).
- [15] E. D'Hondt and P. Panangaden, "The computational power of the W and GHZ states," 2004, *arXiv:quant-ph/0412177*, doi: [10.48550/arXiv.quant-ph/0412177](https://doi.org/10.48550/arXiv.quant-ph/0412177).
- [16] M. Pompili et al., "Realization of a multinode quantum network of remote solid-state qubits," *Science*, vol. 372, no. 6539, pp. 259–264, Apr. 2021, doi: [10.1126/science.abg191](https://doi.org/10.1126/science.abg191).
- [17] J. I. Cirac, P. Zoller, H. J. Kimble, and H. Mabuchi, "Quantum state transfer and entanglement distribution among distant nodes in a quantum network," *Phys. Rev. Lett.*, vol. 78, no. 16, 1997, Art. no. 3221, doi: [10.1103/PhysRevLett.78.3221](https://doi.org/10.1103/PhysRevLett.78.3221).
- [18] L. Childress, J. Taylor, A. S. Sørensen, and M. D. Lukin, "Fault-tolerant quantum repeaters with minimal physical resources and implementations based on single-photon emitters," *Phys. Rev. A*, vol. 72, no. 5, 2005, Art. no. 052330, doi: [10.1103/PhysRevA.72.052330](https://doi.org/10.1103/PhysRevA.72.052330).
- [19] P. Van Loock et al., "Hybrid quantum repeater using bright coherent light," *Phys. Rev. Lett.*, vol. 96, no. 24, 2006, Art. no. 240501, doi: [10.1103/PhysRevLett.96.240501](https://doi.org/10.1103/PhysRevLett.96.240501).
- [20] M. Uphoff, M. Brekenfeld, G. Rempe, and S. Ritter, "An integrated quantum repeater at telecom wavelength with single atoms in optical fiber cavities," *Appl. Phys. B*, vol. 122, pp. 1–15, 2016, doi: [10.1007/s00340-015-6299-2](https://doi.org/10.1007/s00340-015-6299-2).
- [21] X.-M. Hu et al., "Long-distance entanglement purification for quantum communication," *Phys. Rev. Lett.*, vol. 126, no. 1, 2021, Art. no. 010503, doi: [10.1103/PhysRevLett.126.010503](https://doi.org/10.1103/PhysRevLett.126.010503).
- [22] G. Moody et al., "2022 roadmap on integrated quantum photonics," *J. Phys.: Photon.*, vol. 4, no. 1, 2022, Art. no. 012501, doi: [10.1088/2515-7647/ac1ef4](https://doi.org/10.1088/2515-7647/ac1ef4).



- [23] C. H. Bennett, G. Brassard, S. Popescu, B. Schumacher, J. A. Smolin, and W. K. Wootters, "Purification of noisy entanglement and faithful teleportation via noisy channels," *Phys. Rev. Lett.*, vol. 76, no. 5, 1996, Art. no. 722, doi: [10.1103/PhysRevLett.76.722](https://doi.org/10.1103/PhysRevLett.76.722).
- [24] D. Deutsch, A. Ekert, R. Jozsa, C. Macchiavello, S. Popescu, and A. Sanpera, "Quantum privacy amplification and the security of quantum cryptography over noisy channels," *Phys. Rev. Lett.*, vol. 77, no. 13, 1996, Art. no. 2818, doi: [10.1103/PhysRevLett.77.2818](https://doi.org/10.1103/PhysRevLett.77.2818).
- [25] A. S. Cacciapuoti, M. Caleffi, R. Van Meter, and L. Hanzo, "When entanglement meets classical communications: Quantum teleportation for the quantum internet," *IEEE Trans. Commun.*, vol. 68, no. 6, pp. 3808–3833, Jun. 2020, doi: [10.1109/TCOMM.2020.2978071](https://doi.org/10.1109/TCOMM.2020.2978071).
- [26] R. V. Meter, T. D. Ladd, W. J. Munro, and K. Nemoto, "System design for a long-line quantum repeater," *IEEE/ACM Trans. Netw.*, vol. 17, no. 3, pp. 1002–1013, Jun. 2008, doi: [10.1109/TNET.2008.927260](https://doi.org/10.1109/TNET.2008.927260).
- [27] A. Dahlberg et al., "A link layer protocol for quantum networks," in *Proc. ACM Special Int. Group Data Commun.*, 2019, pp. 159–173, doi: [10.1145/3341302.3342070](https://doi.org/10.1145/3341302.3342070).
- [28] W. Kozłowski, A. Dahlberg, and S. Wehner, "Designing a quantum network protocol," in *Proc. 16th Int. Conf. Emerg. Netw. Experiments Technol.*, 2020, pp. 1–16, doi: [10.1145/3386367.3431293](https://doi.org/10.1145/3386367.3431293).
- [29] P. W. Shor, "Algorithms for quantum computation: Discrete logarithms and factoring," in *Proc. 35th Annu. Symp. Foundations Comput. Sci.*, 1994, pp. 124–134, doi: [10.1109/SFCS.1994.365700](https://doi.org/10.1109/SFCS.1994.365700).
- [30] S. B. Bravyi and A. Y. Kitaev, "Quantum codes on a lattice with boundary," 1998, *arXiv:quant-ph/9811052*, doi: [10.48550/arXiv.quant-ph/9811052](https://doi.org/10.48550/arXiv.quant-ph/9811052).
- [31] L. Valentini, D. Forlivesi, and M. Chiani, "Performance analysis of quantum error-correcting surface codes over asymmetric channels," in *Proc. IEEE Int. Conf. Commun.*, 2023, pp. 4175–4181, doi: [10.1109/ICC45041.2023.10279096](https://doi.org/10.1109/ICC45041.2023.10279096).
- [32] D. Forlivesi, L. Valentini, and M. Chiani, "Logical error rates of XZZX and rotated quantum surface codes," *IEEE J. Sel. Areas Commun.*, early access, Mar. 21, 2024, doi: [10.1109/JSAC.2024.3380088](https://doi.org/10.1109/JSAC.2024.3380088).
- [33] M. Chiani, A. Conti, and M. Z. Win, "Piggybacking on quantum streams," *Phys. Rev. A*, vol. 102, no. 1, Jul. 2020, Art. no. 012410, doi: [10.1103/PhysRevA.102.012410](https://doi.org/10.1103/PhysRevA.102.012410).
- [34] P. W. Shor, "Scheme for reducing decoherence in quantum computer memory," *Phys. Rev. A*, vol. 52, Oct. 1995, Art. no. R2493, doi: [10.1103/PhysRevA.52.R2493](https://doi.org/10.1103/PhysRevA.52.R2493).
- [35] R. Laflamme, C. Miquel, J. P. Paz, and W. H. Zurek, "Perfect quantum error correcting code," *Phys. Rev. Lett.*, vol. 77, no. 1, 1996, Art. no. 198, doi: [10.1103/PhysRevLett.77.198](https://doi.org/10.1103/PhysRevLett.77.198).
- [36] M. Grassl, "Bounds on the minimum distance of linear codes and quantum codes," 2007, Accessed: Dec. 20, 2019. [Online]. Available: <http://www.codetables.de>
- [37] P. K. Sarvepalli, A. Klappenecker, and M. Rötteler, "Asymmetric quantum codes: Constructions, bounds and performance," *Proc. Roy. Soc. A: Math., Phys. Eng. Sci.*, vol. 465, no. 2105, pp. 1645–1672, 2009, doi: [10.1098/rspa.2008.0439](https://doi.org/10.1098/rspa.2008.0439).
- [38] M. Chiani and L. Valentini, "Short codes for quantum channels with one prevalent Pauli error type," *IEEE J. Sel. Areas Inf. Theory*, vol. 1, no. 2, pp. 480–486, Aug. 2020, doi: [10.1109/JSAIT.2020.3012827](https://doi.org/10.1109/JSAIT.2020.3012827).
- [39] A. Steane, "Multiple-particle interference and quantum error correction," *Proc. Roy. Soc. London. Ser. A*, vol. 452, no. 1954, pp. 2551–2577, 1996, doi: [10.1098/rspa.1996.0136](https://doi.org/10.1098/rspa.1996.0136).
- [40] A. R. Calderbank and P. W. Shor, "Good quantum error-correcting codes exist," *Phys. Rev. A*, vol. 54, no. 2, 1996, Art. no. 1098, doi: [10.1103/PhysRevA.54.1098](https://doi.org/10.1103/PhysRevA.54.1098).
- [41] A. M. Steane, "Enlargement of Calderbank-Shor-Steane quantum codes," *IEEE Trans. Inf. Theory*, vol. 45, no. 7, pp. 2492–2495, Nov. 1999, doi: [10.1109/18.796388](https://doi.org/10.1109/18.796388).
- [42] S. Muralidharan, L. Li, J. Kim, N. Lütkenhaus, M. D. Lukin, and L. Jiang, "Optimal architectures for long distance quantum communication," *Sci. Rep.*, vol. 6, no. 1, 2016, Art. no. 20463, doi: [10.1038/srep20463](https://doi.org/10.1038/srep20463).
- [43] M. Hein, J. Eisert, and H. J. Briegel, "Multiparty entanglement in graph states," *Phys. Rev. A*, vol. 69, no. 6, 2004, Art. no. 062311, doi: [10.1103/PhysRevA.69.062311](https://doi.org/10.1103/PhysRevA.69.062311).
- [44] M. Hein, W. Dür, J. Eisert, R. Raussendorf, M. Nest, and H.-J. Briegel, "Entanglement in graph states and its applications," 2006, *arXiv:quant-ph/0602096*, doi: [10.48550/arXiv.quant-ph/0602096](https://doi.org/10.48550/arXiv.quant-ph/0602096).
- [45] C. Meignant, D. Markham, and F. Grosshans, "Distributing graph states over arbitrary quantum networks," *Phys. Rev. A*, vol. 100, no. 5, 2019, Art. no. 052333, doi: [10.1103/PhysRevA.100.052333](https://doi.org/10.1103/PhysRevA.100.052333).
- [46] E. Rieffel and W. Polak, "An introduction to quantum computing for non-physicists," *ACM Comput. Surv.*, vol. 32, no. 3, pp. 300–335, 2000, doi: [10.1145/367701.367709](https://doi.org/10.1145/367701.367709).
- [47] M. A. Nielsen and I. L. Chuang, *Quantum Computation and Quantum Information*. New York, NY, USA: Cambridge Univ. Press, 2010, doi: [10.1017/CBO9780511976667](https://doi.org/10.1017/CBO9780511976667).
- [48] R. F. Werner, "Quantum states with Einstein-Podolsky-Rosen correlations admitting a hidden-variable model," *Phys. Rev. A*, vol. 40, no. 8, 1989, Art. no. 4277, doi: [10.1103/PhysRevA.40.4277](https://doi.org/10.1103/PhysRevA.40.4277).
- [49] Y.-S. Zhang, Y.-F. Huang, C.-F. Li, and G.-C. Guo, "Experimental preparation of the Werner state via spontaneous parametric down-conversion," *Phys. Rev. A*, vol. 66, no. 6, 2002, Art. no. 062315, doi: [10.1103/PhysRevA.66.062315](https://doi.org/10.1103/PhysRevA.66.062315).
- [50] S. Das, M. S. Rahman, and M. Majumdar, "Design of a quantum repeater using quantum circuits and benchmarking its performance on an IBM quantum computer," *Quantum Inf. Process.*, vol. 20, 2021, Art. no. 245, doi: [10.1007/s1128-021-03189-8](https://doi.org/10.1007/s1128-021-03189-8).
- [51] W. Dür, H.-J. Briegel, J. I. Cirac, and P. Zoller, "Quantum repeaters based on entanglement purification," *Phys. Rev. A*, vol. 59, no. 1, 1999, Art. no. 169, doi: [10.1103/PhysRevA.59.169](https://doi.org/10.1103/PhysRevA.59.169).
- [52] W. Dür and H. J. Briegel, "Entanglement purification and quantum error correction," *Rep. Prog. Phys.*, vol. 70, no. 8, 2007, Art. no. 1381, doi: [10.1088/0034-4885/70/8/R03](https://doi.org/10.1088/0034-4885/70/8/R03).
- [53] H. H. S. Chittoor and O. Simeone, "Learning quantum entanglement distillation with noisy classical communications," in *IEEE Int. Conf. Acoust., Speech Signal Process.*, 2023, pp. 1–5, doi: [10.1109/ICASSP49357.2023.10097202](https://doi.org/10.1109/ICASSP49357.2023.10097202).
- [54] C. Macchiavello, "On the analytical convergence of the QPA procedure," *Phys. Lett. A*, vol. 246, no. 5, pp. 385–388, 1998, doi: [10.1016/S0375-9601\(98\)00550-7](https://doi.org/10.1016/S0375-9601(98)00550-7).
- [55] S. Krastanov, V. V. Albert, and L. Jiang, "Optimized entanglement purification," *Quantum*, vol. 3, 2019, Art. no. 123, doi: [10.22331/q-2019-02-18-123](https://doi.org/10.22331/q-2019-02-18-123).
- [56] K. Goodenough et al., "Near-term  $n$  to  $k$  distillation protocols using graph codes," *IEEE J. Sel. Areas Commun.*, 2024, doi: [10.1109/JSAC.2024.3380094](https://doi.org/10.1109/JSAC.2024.3380094).
- [57] D. Gottesman, "An introduction to quantum error correction and fault-tolerant quantum computation," 2009, *arXiv:0904.2557*, doi: [10.48550/arXiv.0904.2557](https://doi.org/10.48550/arXiv.0904.2557).
- [58] D. J. MacKay, G. Mitchison, and P. L. McFadden, "Sparse-graph codes for quantum error correction," *IEEE Trans. Inf. Theory*, vol. 50, no. 10, pp. 2315–2330, Oct. 2004, doi: [10.1109/TIT.2004.834737](https://doi.org/10.1109/TIT.2004.834737).
- [59] N. H. Nickerson, Y. Li, and S. C. Benjamin, "Topological quantum computing with a very noisy network and local error rates approaching one percent," *Nature Commun.*, vol. 4, no. 1, Apr. 2013, Art. no. 1756, doi: [10.1038/ncomms2773](https://doi.org/10.1038/ncomms2773).
- [60] A. S. Cacciapuoti, M. Caleffi, R. V. Meter, and L. Hanzo, "When entanglement meets classical communications: Quantum teleportation for the quantum Internet," *IEEE Trans. Commun.*, vol. 68, no. 6, pp. 3808–3833, Jun. 2020, doi: [10.1109/TCOMM.2020.2978071](https://doi.org/10.1109/TCOMM.2020.2978071).
- [61] S. D. Barrett and P. Kok, "Efficient high-fidelity quantum computation using matter qubits and linear optics," *Phys. Rev. A*, vol. 71, no. 6, 2005, Art. no. 060310, doi: [10.1103/PhysRevA.71.060310](https://doi.org/10.1103/PhysRevA.71.060310).
- [62] A. M. Steane, "Error correcting codes in quantum theory," *Phys. Rev. Lett.*, vol. 77, no. 5, 1996, Art. no. 793, doi: [10.1103/PhysRevLett.77.793](https://doi.org/10.1103/PhysRevLett.77.793).
- [63] H.-J. Briegel, W. Dür, J. I. Cirac, and P. Zoller, "Quantum repeaters: The role of imperfect local operations in quantum communication," *Phys. Rev. Lett.*, vol. 81, no. 26, 1998, Art. no. 5932, doi: [10.1103/PhysRevLett.81.5932](https://doi.org/10.1103/PhysRevLett.81.5932).

Open Access funding provided by 'Alma Mater Studiorum - Università di Bologna' within the CRUI CARE Agreement